Science Arts & Métiers (SAM)

is an open access repository that collects the work of Arts et Métiers Institute of Technology researchers and makes it freely available over the web where possible.

This is an author-deposited version published in: https://sam.ensam.eu
Handle ID: .http://hdl.handle.net/10985/8588

To cite this version :

Juan WANG, Florent RAVELET, Farid BAKIR - Experimental comparison between a counter-rotating axial-flow fan and a conventional rotor-stator stage - In: 10th European Turbomachinery Conference, Lappeenranta, Finland, Finland, 2013 - 10th European Turbomachinery Conference, Lappeenranta : Finlande - 2013

Any correspondence concerning this service should be sent to the repository Administrator : scienceouverte@ensam.eu

Arts et Métiers Institute of Technology

hal-00795006, version 1 - 27 Feb 2013

Experimental comparison between a counter-rotating axial-flow fan and a conventional rotor-stator stage

J. Wang - F. Ravelet - F. Bakir

DynFluid Lab., Arts et Metiers ParisTech, 151 boulevard de l'Hôpital, 75013 Paris, France,
florent.ravelet@ensam.eu

ABSTRACT

Based on the requirement of energy consumption level and weight and dimension restriction, compact axial machines are highly demanded in many industrial fields. The counter-rotating axial-flow fans could be a promising way to achieve these requirements. Because of the reduction of rotational speed and a better homogenization of the flow downstream of the rear rotor, these machines may have very good aerodynamic performances. However, they are rarely used in subsonic applications, mainly due to poor knowledge of the aerodynamics in the mixing area between the two rotors, where very complex structures are produced by the interaction of highly unsteady flows. The purpose of the present work is to compare the global performances (static pressure rise and static efficiency) and the wall pressure fluctuations downstream of the first rotor for three different stages operating at the same point: a single subsonic axial-flow fan, a conventional rotor-stator stage and a counter-rotating system that have been designed with in-house tools. The counter-rotating system allows large savings of energy with respect to the other two systems, for lower rotation rates and by adjusting the distance between the two rotors, a solution with comparable wall pressure fluctuations levels for the three systems is found.

NOMENCLATURE

Symbols

D	Pipe diameter
f	blade passing frequency
N	rotational rate (rpm)
P_{atm}	atmospheric pressure
P_s	static pressure
Q	Volumetric flow rate
s	axial distance
W	Power
z	axial coordinate
ΔP_s	static pressure rise
η_s	static efficiency
ϕ	volumetric flow rate coefficient
ω	angular velocity
Ψ_s	static head coefficient
ρ	density of the air
τ	torque
θ	ratio of angular velocities

Acronyms

CRS	counter-rotating system
FR	front rotor
RR	rear rotor
R1	front rotor alone
RSS	rotor-stator stage

INTRODUCTION

Nowadays, a revival of industrial interest for counter-rotating axial machines can be observed for various applications in subsonic regimes, as for instance fans and pumps, operating in ducted or free-flow configurations (Cho et al., 2009; Shigemitsu et al., 2009, 2010; Xu et al., 2009; Yoshihiko, 2003).

hal-00795006, version 1 - 27 Feb 2013

Counter-rotating axial-flow fans for electronic devices cooling application are for instance developed by SANYO DENKI (manufacturer of fans) with various diameters. According to Yoshihiko (2003), these products have the advantages of large air volume, high static pressure while lower noise and power consumption, compared to 2 conventional fans used in series. For the same type of industrial application, Shigemitsu et al. (2010) have shown with numerical studies that counter-rotating axial small-size fans provided higher pressure and efficiency than one single rotor. However, detailed experiments and analysis are still demanded to reveal the physical mechanisms that improve their efficiency compared to the conventional facilities.

The general idea of a counter-rotating system is that two rotors (front and rear) are rotating in opposite directions. The energy in the tangential velocity component of the flow after the first rotor is usually wasted in the wake (Dron, 2008). At the inlet of the rear rotor of a counter-rotating fan stage, this tangential velocity contributes to higher relative velocity, then it diffuses in the second rotor and is moreover converted to static pressure rise. Compared to a conventional rotor-stator stage, the rear rotor not only recovers the static head but also supplies energy to the fluid.

Given all the advantages indicated above, the counter-rotating system attracts attention of a large number of researchers. An original method to design such a system has been developped in the DynFluid Laboratory and has been validated on a first prototype: CRS (Nouri et al., 2013). In this experiment, the rotors operate in a duct of diameter $D = 380$ mm, the ratio $\theta = \frac{N_{RR}}{N_{FR}}$ of the rotation rates of the two rotors can be varied, and the axial distance s between the front rotor and the second rotor can be varied in a wide range (see Fig. 1).

The main results of this study are:

- the maximum of the peak static efficiency of CRS is $67 \pm 1\%$ whilst the peak static efficiency of the front rotor alone is $45 \pm 1\%$;
- at the design angular velocity ratio $\theta = 0.9$ the overall performances are not significantly

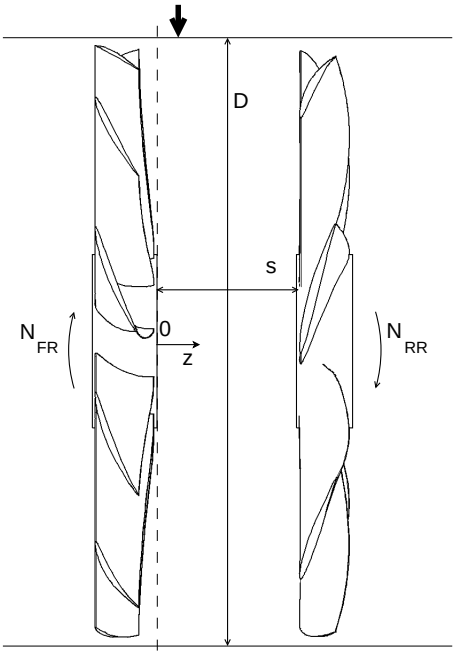

Figure 1: Sketch of the CRS arrangement that is considered in the present paper, showing the coordinate system and the main dimensions. The front rotor (FR) is on the left, and the rear rotor (RR) is on the right. The bold arrow stands for the microphone (position $z = 5$ mm).

hal-00795006, version 1 - 27 Feb 2013

affected by a variation of the axial distance in the range $s = \in [10; 50]$ mm, with s the distance between the trailing edge of the front rotor and the leading edge of the rear rotor;

- However, at $\theta = 0.9$, the pressure rise is decreased by 5% and the efficiency decreases from $65 \pm 1\%$ to $63 \pm 1\%$ when s is increased from 10 to 180 mm;
- at small axial distances ($s < 50$ mm), the analysis of the power spectral density for wall pressure fluctuations and of the radial profiles of the average velocity confirm that the rear rotor does significantly affect the flow field in the interaction area.

The main objective of the present study is to experimentally detail the differences between CRS, a conventional single rotor stage (R1) and a conventional rotor-stator stage (RSS). To achieve this target, a first series of experiments are carried out on a single axial-flow fan (R1). Then a stator is designed to fit with this rotor to form RSS and finally, the second counter-rotating rotor is used to form the counter-rotating stage (CRS). The experimental set-up is first briefly described. Then, the overall performances of the three systems are compared. In order to compare the levels and spectra of the wall pressure fluctuations, a seek for operating conditions of the three systems that lead to the same given output aerodynamic power is then performed. Finally, the effects of the axial distance s for RSS and CRS both on the global performances and on the pressure fluctuations levels and spectra are studied.

EXPERIMENTAL SET-UP AND MEASUREMENTS METHOD

The experimental investigations of the three configurations (R1, CRS and RSS) are performed on a normalized experimental test-bench: AERO^{2}FANS, built for this purpose in the DynFluid Laboratory. The design points of R1 and of CRS are respectively a total pressure rise of 260 Pa and 420 Pa at a nominal volumetric flow rate $Q = 1$ m^3.s^{-1} and for rotation rates $N_{FR} = 2000$ rpm and $\theta = 0.9$. More details about the test bench and those two configurations are given in the article of Nouri et al. (2013).

In the present paper, the static pressure rise is defined according to the ISO-5801 standard as the difference between the static pressure downstream of the studied machine and the total pressure at the inlet (atmospheric pressure): $\Delta P_s = P_{sRR2} - P_{atm}$. This value is obtained by averaging the results of four pressure taps placed downstream of a flow straightener, then corrected with the pressure drop of the circuit that is measured without the rotors. The static efficiency is defined as $\eta_s = \frac{\Delta P_s Q}{(\tau_{FR}\omega_{FR})+(\tau_{RR}\omega_{RR})}$. The torque τ is measured by the drivers of the DC brushless motors and has been calibrated against a rotating torquemeter. The casing wall pressure fluctuations are recorded by a 40BP pressure microphone, which has been calibrated by an acoustic calibrator. The sampling frequency for the signal of the wall pressure fluctuations is 6 kHz. The power spectral density and the total average power of the pressure fluctuations are expressed in dB.Hz^{-1} and dB with a pressure reference of 1 Pa. The axial distance between the two rotors s and the position of the microphone z are defined in Fig. 1.

RESULTS AND DISCUSSION

Comparison of the overall performances of R1, RSS and CRS

To compare the overall performance of the three configurations (R1, RSS, CRS), some working conditions are first set: the axial distance for RSS is $s = 15$ mm and for CRS it is $s = 10$ mm, which corresponds to 17% of the chord of FR at mid-span. In the following, the θ ratio of CRS is always set to $\theta = 1$ and the symbol N thus stands for the rotation rate of the rotor(s) for R1, RSS and CRS. The static head coefficient defined by $\Psi_s = \frac{\Delta P_s/\rho}{(N/60)^2 D^2}$ as a function of the volumetric flow coefficient defined by $\phi = \frac{Q}{(N/60)D^3}$ and the static efficiency η_s as a function of ϕ are plotted in Fig. 2. The

hal-00795006, version 1 - 27 Feb 2013

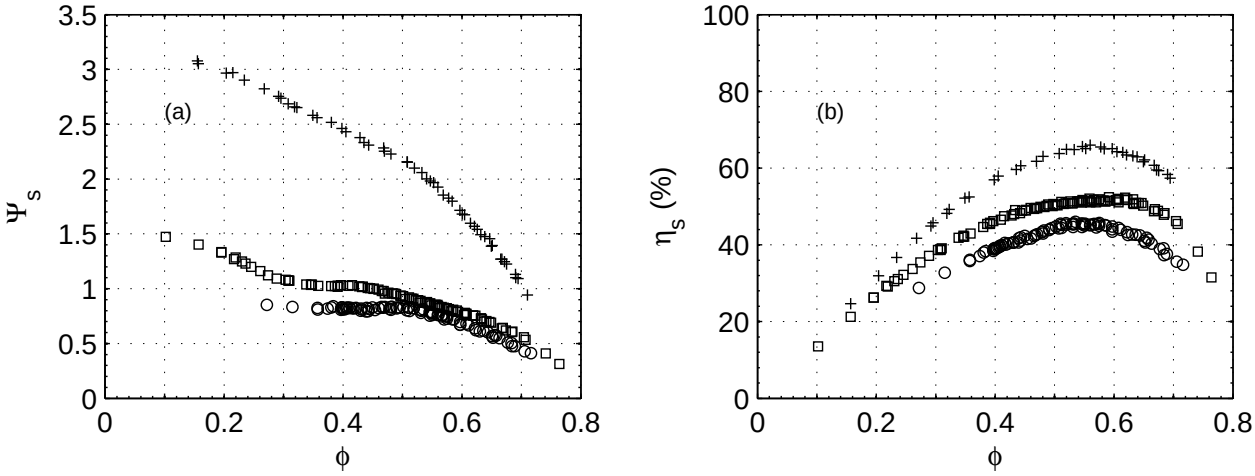

Figure 2: Dimensionless characteristics of the three systems: R1 (○), RSS at $s = 15$ mm (□) and CRS at $s = 10$ mm and $\theta = 1$ (+). (a): Static head coefficient Ψ_s *vs.* volumetric flow rate coefficient ϕ. (b): Static efficiency η_s *vs.* flow coefficient ϕ.

data reported in this figure have been obtained at various rotation rates: respectively $N = 2100$ and 2300 rpm for R1, $N = 2000$, 2100 and 2200 rpm for RSS, and $N = 1600$ and 1800 rpm for CRS. The Reynolds numbers based on the relative inlet velocity and on the chord at mid-span are all greater than 2.4×10^5 (Nouri et al., 2013).

The different curves fairly collapse for each system: the dimensionless coefficients do not depend on the Reynolds number, which is a classical result for developped turbulent flows (Tennekes and Lumley, 1972).

It can be moreover observed that the slope of the Ψ_s *vs.* ϕ curve is steeper for CRS than for R1 and RSS, as noticed by Shigemitsu et al. (2009): this feature can be explained close to the nominal volumetric flow rate with a theory based on the energy and angular momentum balances for perfect fluid (Euler's equation of turbomachinery). The present results moreover show that, contrary to what is observed for the single rotor R1 or the conventional rotor-stator stage RSS, the characteristic curve of CRS has a large negative slope even at very low volumetric flow rates which corresponds to a very good operating stability.

The maximum efficiency for R1 is $45 \pm 1\%$, while it is $51 \pm 1\%$ for RSS and $66 \pm 1\%$ for CRS. The gain in peak-efficiency brought by the use of the stator is approximately $+6$ percentage-points with respect to R1, which is a classical value according to Moreau and Bakir (2002). The gain in efficiency brought by the use of a counter-rotating rotor —roughly $+21$ percentage-points— is thus much higher.

Comparison of the systems when delivering the same given output aerodynamic power

Overall performances

In view of comparing both the global performances and the wall pressure fluctuations for the different systems R1, RSS and CRS in a dimensional point of view, three working conditions are now studied. The rotation rates of the three systems are adjusted such that the same aerodynamic output power is obtained. In other words, a seek for points such that $\Delta P_s Q = constant$ has been performed. The flow conditions and the corresponding operating conditions for each system are given in Tab. 1 for those three "crosspoints".

The crosspoint 1 corresponds to an operating point where CRS is working at a nominal flow

hal-00795006, version 1 - 27 Feb 2013

Cross points	Parameters	R1	RSS	CRS
Crosspoint 1	Q (m^3.s^{-1})		0.87	
	ΔP_s (Pa)		212	
	N (rpm)	2300	2100	1600
	η_s	40%	49%	66%
	W (W)	461	375	279
Crosspoint 2	Q (m^3.s^{-1})		0.95	
	ΔP_s (Pa)		177	
	N (rpm)	2100	2000	1600
	η_s	44%	51%	66%
	W (W)	380	328	256
Crosspoint 3	Q (m^3.s^{-1})		1.08	
	ΔP_s (Pa)		209	
	N (rpm)	2300	2200	1800
	η_s	45%	51%	61%
	W (W)	500	443	369

Table 1: Operating conditions of the three systems for the crosspoints 1, 2 and 3 ($\rho = 1.21$ kg.m^{-3}).

rate, the crosspoint 2 corresponds to RSS working at a nominal flow rate and the crosspoint 3 to R1 at a nominal point. It is obvious that to reach the same pressure rise at the same volumetric flow rate, CRS always requires much lower rotational velocity compared to R1 and RSS: in the worst case (crosspoint 3), the rotation rate of CRS is respectively 78% and 82% of that of R1 and RSS. In addition, the static efficiency of CRS is 16 percentage-points higher than that of R1 and 10 percentage-points higher than that of RSS in the worst case (crosspoint 3 corresponding to an overflow rate of 114% for CRS). Besides, at the three crosspoints, the mechanical power consumed by CRS is respectively 40%, 32% and 26% lower than that of R1. In another way, it could be concluded that CRS could provide higher pressure rise and air volumetric flow rate at a given power consumption, consequently allowing a decrease of the fan diameter and of the rotational speed.

Comparison of wall pressure fluctuations at crosspoint 1 and small axial distances

The figure 3 shows the power spectral density of the wall pressure fluctuations measured at the same operating point (crosspoint 1 in Tab. 1) for the three configurations and for the same s as in the previous paragraph. These power spectra are characterized by a broadband noise superimposed to a series of discrete frequency peaks. It is obvious that the spectrum for CRS presents much more peaks. These peaks can be classified into three categories: front rotor blade passing frequency f_{FR} and its harmonics ($\circ$), rear rotor blade passing frequency f_{RR} and its harmonics ($\square$) and the frequencies resulting from the interactions between the two aforementioned modes, that consist of linear combinations $mf_{FR} + nf_{RR}$ where $m, n \in \mathbb{Z}^*$. Results observed by Nouri et al. (2013) on the same facility at a different θ are in accordance with this theory for the CRS tonal noise. The additional peaks for CRS are due to the potential influence of the rear rotor on the front one, and to the influence of the front rotor on the rear rotor: both vortex shedding and viscous wakes impact the second rotor when the axial distance is small (Blandeau, 2011).

The tonal peaks corresponding to FR for CRS are lower than those for the R1 and RSS systems which is consistent with its lower rotation rate. However, the tonal peaks corresponding to RR are on the one hand larger than that of FR, which is consistent with the higher loading of RR's blades (Nouri et al., 2013) and in addition are even about twice as large as the FR peaks of R1 and RSS. Ultimately,

hal-00795006, version 1 - 27 Feb 2013

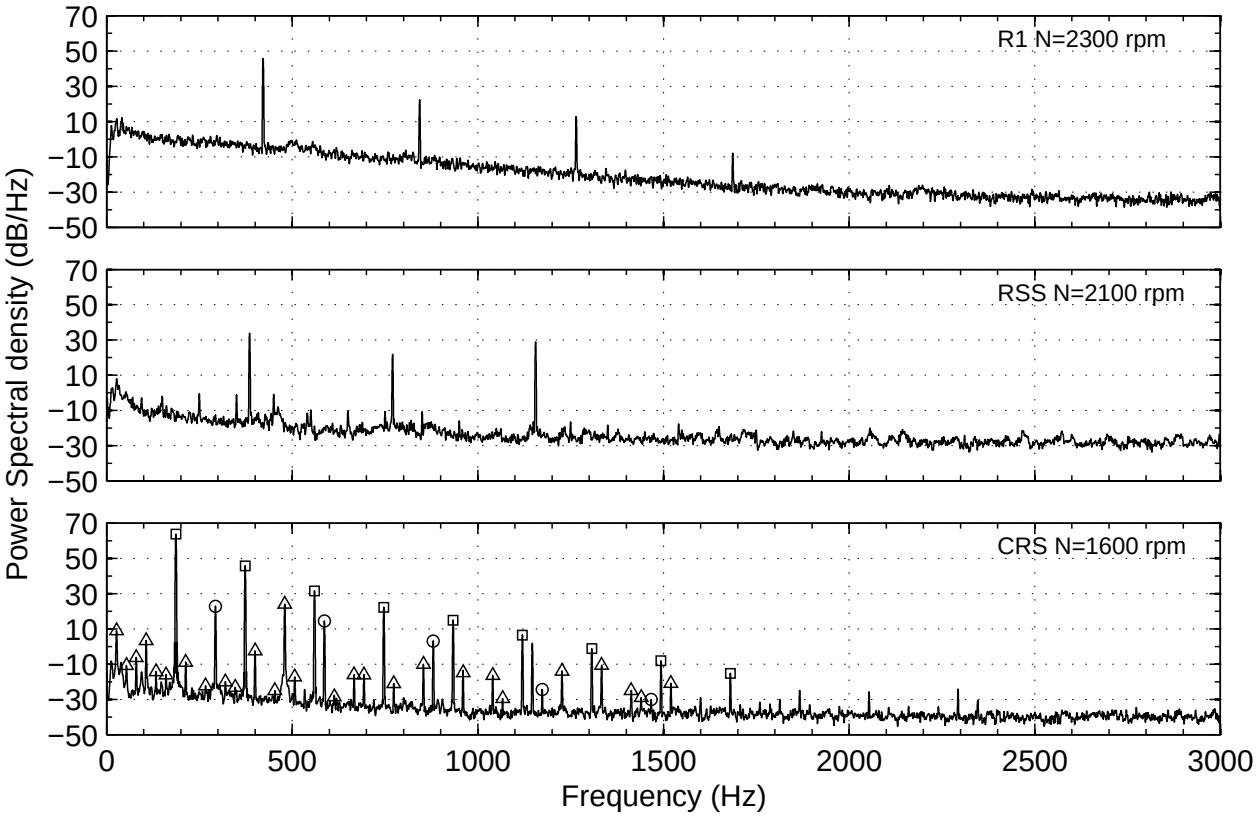

Figure 3: Power spectral density of the wall pressure fluctuations recorded at $z = +5$ mm downstream of FR under crosspoint 1 conditions (see Tab. 1). For CRS, the $\circ$ stand for the blade passing frequency of FR and its harmonics, the $\square$ stand for the blade passing frequency of RR and its harmonics, and the Δ stand for the interactions of these frequencies.

hal-00795006, version 1 - 27 Feb 2013

the total level of the wall pressure fluctuations, *i.e.* the average power, is respectively 26.9 ± 0.2 dB, 30.8 ± 0.2 dB and 37.4 ± 0.2 dB for RSS, R1 and CRS. As the wall pressure fluctuations may be in close relation to the acoustic sources (Joongnyon and Hyung, 2006), CRS at $s = 10$ mm may thus be much noisier than RSS for the same aerodynamic output power.

Influence of the axial distance s on RSS and CRS

The figure 4 presents the influence of the axial distance s on the performances of RSS and CRS. The performances of RSS for $s = 5$, 15 and 55 mm are plotted in Fig. 4(a-b) and that of CRS at $\theta = 1$ for $s = 10$ and 50 mm are plotted in Fig. 4(c-d). For both systems, the pressure rise is unaffected at nominal and overflow rates and slightly decreases with increasing s at partial flow rates. As explained by van Zante et al. (2002), viscous loss effects in the wake modify inlet angles for the second rotor and then less energy is recovered by the second —stationary or rotating— blade cascade for increased axial distance. Concerning the static efficiency, the small differences that can be observed are within the measurement uncertainty. This infers that the axial distance s does not have obvious influence on the global performances of RSS and CRS, in the studied range of axial distances that corresponds to $9\% \leq s \leq 95\%$ (in percentage of the chord of FR at mid-span).

The figure 5 presents the influence of the axial distance s on the wall pressure fluctuations downstream of FR for RSS and CRS. Concerning RSS, the increase of axial distance from $s = 15$ to $s = 55$ mm only leads to slight qualitative modifications of the spectrum with a low attenuation of the fourth harmonic. The total average power of the signal decreases from 28.6 ± 0.2 to 27.8 ± 0.2 dB. On

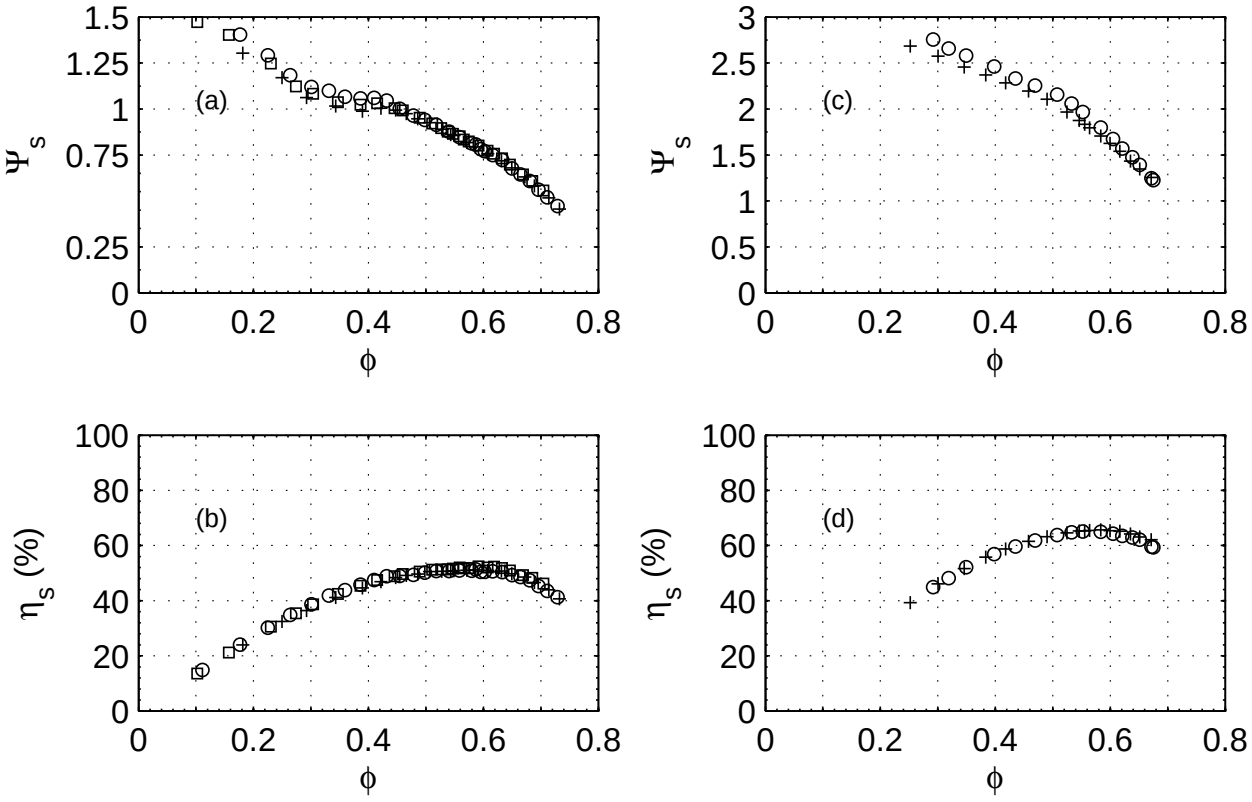

Figure 4: Influence of the axial distance on the performances. (a-b): RSS, Ψ_s and η_s *vs.* ϕ for ($\circ$): $s = 5$ mm, ($\square$): $s = 15$ mm and ($+$): $s = 55$ mm. (c-d): CRS, Ψ_s and η_s *vs.* ϕ for ($\circ$): $s = 10$ mm and ($+$): $s = 50$ mm.

hal-00795006, version 1 - 27 Feb 2013

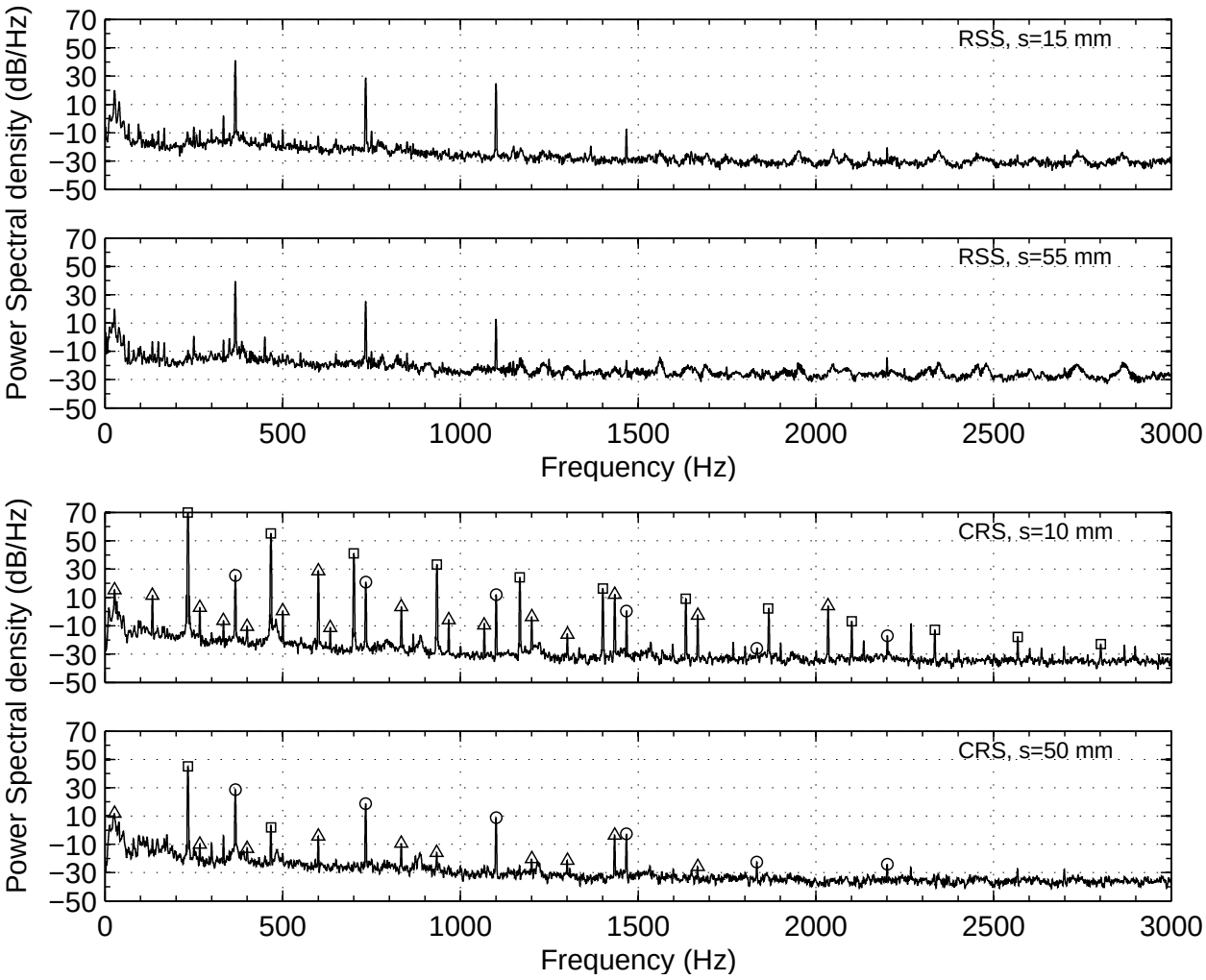

Figure 5: Power spectral density of the wall pressure fluctuations recorded at $z = +5$ mm downstream of FR for RSS and CRS rotating at $N = 2000$ rpm for various axial distances. The operating point is the nominal point of each case. The $\circ$ stand for the blade passing frequency of FR and its harmonics, the $\square$ stand for the blade passing frequency of RR and its harmonics, and the Δ stand for the interactions of these frequencies.

hal-00795006, version 1 - 27 Feb 2013

the opposite, one can observe a huge effect of the increase in axial distance on the spectral content for CRS. First of all, the peaks corresponding to the RR are strongly attenuated and only the fundamental (f_{RR}) and the second harmonic ($2f_{RR}$) are present for $s = 50$ mm while up to 10 harmonics are visible for $s = 10$ mm. Similarly, the interaction peaks are considerably weakened. On the other hand, the peaks corresponding to FR remain unchanged. Ultimately, the total average power is lowered from 42.0 ± 0.2 to 30.3 ± 0.2 dB. It can be concluded that increasing the axial distance would have more influence on CRS than on RSS in terms of wall pressure fluctuations and thus, the axial distance would be an efficient optimization parameter regarding the noise reduction of low-speed counter-rotating axial-flow fans.

CONCLUSIONS

Experimental investigations of the differences in terms of overall performances and wall pressure fluctuations between a single rotor, a conventional rotor-stator stage and a counter-rotating system have been performed. The results can be summarized as follows:

1. The characteristic curve of the counter-rotating system is significantly steeper than that of the single rotor and of the conventional rotor-stator stage and is still significantly negative at very low partial flow rates. This improves the operating stability compared to the conventional configurations.

2. At a given power consumption, the counter-rotating system could produce a much larger pressure rise and efficiency, with a lower rotation rate. The gains in efficiency and in rotation rate with respect to the rotor-stator stage are at least of the order of $+10$ percentage-points and -20% respectively.

3. The study of the wall pressure fluctuations for a small axial distance between the two rotors shows that for the same output aerodynamic power, though CRS is rotating more slowly, it may still be much noisier than R1 and RSS.

4. A slight increase in the axial distance could nonetheless be a very efficient way to cope with this problem, as the overall performances are hardly affected but the average power of wall pressure fluctuations is strongly reduced.

The future works that are now undertaken are first, to design different counter-rotating systems that all have the same design point and differ in the repartition of the load between the two rotors, and on the radial distribution of the Euler work on the first rotor, and also to build a small-scale CRS in order to study its far-field acoustic radiation under anechoic conditions.

References

V. Blandeau. *Aerodynamic Broadband Noise from Contra-Rotating Open Rotors*. PhD thesis, University of southampton, 2011.

L.-S. Cho, B.-J. Cha and J.-S. Cho. Experimental study on the three-dimensional unsteady flow characteristics of the counter-rotating axial flow fan. *Journal of Fluid Science and Technology*, 4: 200–209, 2009.

S. Dron. Toward acare 2020: Innovative engine architectures to achieve the environmantal goals? In *26th International Congress of The Aeronautical Sciences*, pages ICAS 2008–4.2.2, 2008.

K. Joongnyon and J.S. Hyung. Wall pressure fluctuations and flow-induced noise in a turbulent boundary layer over a bump. *J. Fluid Mech.*, 558:79–102, 2006.

hal-00795006, version 1 - 27 Feb 2013

S. Moreau and F. Bakir. Efficient stator designed for automotive engine cooling fan systems. In *ASME 2002 Fluids Engineering Division Summer Meeting*, pages FEDSM02–31318, 2002.

H. Nouri, A. Danlos, F. Ravelet, F. Bakir, and C. Sarraf. Experimental study of the instationary flow between two ducted counter-rotating rotors. *Journal of Engineering for Gas Turbines and Power*, 135:022601, 2013.

D.S. Pundhir and P.B. Sharma. A study of aerodynamic performance of a contra-rotating axial compressor stage. *Defence Science Journal*, 42:191–199, 1992.

T. Shigemitsu, A. Furukawa, S. Watanabe, K. Okuma, and J. Fukutomi. Internal flow measurement with ldv at design point of contra-rotating axial flow pump. *Journal of Fluid Science and Technology*, 4:723–734, 2009.

T. Shigemitsu, J. Fukutomi, and Y. Okabe. Performance and flow condition of small-sized axial fan and adoption of contra-rotating rotors. *Journal of Thermal Science*, 19:1–6, 2010.

H. Tennekes and J. L. Lumley. *A First Course in Turbulence*. MIT Press, Cambridge, 1972.

J. Xu, C. Tan, H. Chen, Y. Zhu and D. Zhang. Influence of tip clearance on performance of a contra-rotating fan. *Journal of Thermal Science*, 18:207–214, 2009.

A. Yoshihiko. Cooling system technology that changes the conventional trend. Technical report, SANYO DENKI, 2003.

D. E. van Zante, J. J. Adamczyk, A. J. Strazisar, and T. H. Okiishi. Wake recovery performance benefit in a high-speed axial compressor. *Journal of Turbomachinery*, 124:275–284, 2002.